

1 **Spring temperature variability over Turkey since 1800 CE reconstructed**
2 **from a broad network of tree-ring data**

3

4 **Nesibe Köse^{(1)*}, H. Tuncay Güner⁽¹⁾, Grant L. Harley⁽²⁾, Joel Guiot⁽³⁾**

5

6 ⁽¹⁾Istanbul University, Faculty of Forestry, Forest Botany Department 34473 Bahçeköy-Istanbul,
7 Turkey

8 ⁽²⁾University of Southern Mississippi, Department of Geography and Geology, 118 College
9 Drive Box 5051, Hattiesburg, Mississippi, 39406, USA

10 ⁽³⁾ Aix-Marseille Université, CNRS, IRD, CEREGE UM34, ECCOREV, 13545 Aix-en-
11 Provence, France

12

13

14

15

16

17 *Corresponding author. Fax: +90 212 226 11 13

18 E-mail address: nesibe@istanbul.edu.tr

19

20 **Abstract**

21 The 20th century was marked by significant decreases in spring temperature ranges and increased
22 nighttime temperatures throughout Turkey. The meteorological observational period in Turkey,
23 which starts *ca.* 1929 CE, is too short for understanding long-term climatic variability. Hence,
24 the historical context of this gradual warming trend in spring temperatures is unclear. Here we
25 use a network of 23 tree-ring chronologies to provide a high-resolution spring (March–April)
26 temperature reconstruction over Turkey during the period 1800–2002. The reconstruction model
27 accounted for 67% (Adj. $R^2 = 0.64$, $p \leq 0.0001$) of the instrumental temperature variance over the
28 full calibration period (1930–2002). During the pre-instrumental period (1800–1929) we captured
29 more cold events ($n = 23$) than warm ($n = 13$), and extreme cold and warm events were typically
30 of short duration (1–2 years). Compared to coeval reconstructions of precipitation in the region,
31 our results are similar with durations of extreme wet and dry events. The reconstruction is
32 punctuated by a temperature increase during the 20th century; yet extreme cold and warm events
33 during the 19th century seem to eclipse conditions during the 20th century. During the 19th
34 century, annual temperature ranges are more volatile and characterized by more short-term
35 fluctuations compared to the 20th century. During the period 1900–2002, our reconstruction
36 shows a gradual warming trend, which includes the period during which diurnal temperature
37 ranges decreased as a result of increased urbanization in Turkey.

38

39 **KEYWORDS:** Dendroclimatology, Climate reconstruction, *Pinus nigra*, Principle component
40 analysis, Spring temperature.

41 **1 Introduction**

42

43 Significant decreases in spring diurnal temperature ranges (DTR) occurred throughout Turkey
44 from 1929 to 1999 (Turkes & Sumer 2004). This decrease in spring DTRs was characterized by
45 day-time temperatures that remained relatively constant while a significant increase in night-time
46 temperatures were recorded over western Turkey and were concentrated around urbanized and
47 rapidly-urbanizing cities. The historical context of this gradual warming trend in spring
48 temperatures is unclear as the high-quality meteorological records in Turkey, which start in
49 1929, are relatively short for understanding long-term climatic variability.

50

51 Tree rings have shown to provide useful information about the past climate of Turkey and were
52 used intensively during the last decade to reconstruct precipitation in the Aegean (, Griggs et al.
53 2007), Black Sea (Akkemik et al. 2005, 2008; Martin-Benitto et al. 2016), Mediterranean regions
54 (Touchan et al. 2005a), as well as the Sivas (D'Arrigo & Cullen 2001), southwestern (Touchan et
55 al. 2003, Touchan et al. 2007; Köse et al. 2013), south-central (Akkemik & Aras 2005) and
56 western Anatolian (Köse et al. 2011) regions of Turkey. These studies used tree rings to
57 reconstruct precipitation because available moisture is often found to be the most important
58 limiting factor that influences radial growth of many tree species in Turkey. These studies
59 revealed past spring-summer precipitation, and described past dry and wet events and their
60 duration. Recently, Heinrich et al. (2013) provided a winter-to-spring temperature proxy for
61 Turkey from carbon isotopes within the growth rings of *Juniperus excelsa* since AD 1125. Low-
62 frequency temperature trends corresponding to the Medieval Climatic Anomaly and Little Ice
63 Age were identified in the record, but the proxy failed to identify the recent warming trend

64 during the 20th century. In this study, we present a tree-ring based spring temperature
65 reconstruction from Turkey and compare our results to previous reconstructions of temperature
66 and precipitation to provide a more comprehensive understanding of climate conditions during
67 the 19th and 20th centuries.

68

69 **2 Data and Methods**

70 2.1 Climate of the Study Area

71

72 The study area, which spans 36–42° N and 26–38° E, was based on the distribution of available
73 tree-ring chronologies. This vast area covers much of western Anatolia and includes the western
74 Black Sea, Marmara, and western Mediterranean regions. Much of this area is characterized by a
75 Mediterranean climate that is primarily controlled by polar and tropical air masses (Türkeş 1996,
76 Deniz et al. 2011). In winter, polar fronts from the Balkan Peninsula bring cold air that is
77 centered in the Mediterranean. Conversely, the dry, warm conditions in summer are dominated
78 by weak frontal systems and maritime effects. Moreover, the Azores high-pressure system in
79 summer and anticyclonic activity from the Siberian high-pressure system often cause below
80 normal precipitation and dry sub-humid conditions over the region (Türkeş 1999, Deniz et al.
81 2011). In this Mediterranean climate, annual mean temperature and precipitation range from 3.6
82 °C to 20.1 °C and from 295 to 2220 mm, respectively, both of which are strongly controlled by
83 elevation (Deniz et al. 2011).

84

85

86

87

88 2.2 Development of tree-ring chronologies

89

90 To investigate past temperature conditions, we used a network of 23 tree-ring site chronologies
91 (Fig. 1). Fifteen chronologies were produced by previous investigations (Mutlu et al. 2011,
92 Akkemik et al. 2008, Köse et al. unpublished data, Köse et al. 2011, Köse et al. 2005) that
93 focused on reconstructing precipitation in the study area. In addition, we sampled eight new
94 study sites and developed tree-ring time series for these areas (Table 1). Increment cores were
95 taken from living *Pinus nigra* Arn. and *Pinus sylvestris* L. trees and cross-sections were taken
96 from *Abies nordmanniana* (Steven) Spach and *Picea orientalis* (L.) Link trunks.

97

98 Samples were processed using standard dendrochronological techniques (Stokes & Smiley 1968,
99 Orvis & Grissino-Mayer 2002, Speer 2010). Tree-ring widths were measured, then visually
100 crossdated using the list method (Yamaguchi 1991). We used the computer program COFECHA,
101 which uses segmented time-series correlation techniques, to statistically confirm our visual
102 crossdating (Holmes 1983, Grissino-Mayer 2001). Crossdated tree-ring time series were then
103 standardized by fitting a 67% cubic smoothing spline with a 50% cutoff frequency to remove
104 non-climatic trends related to the age, size, and the effects of stand dynamics using the ARSTAN
105 program (Cook 1985, Cook et al. 1990a). These detrended series were then pre-whitened with
106 low-order autoregressive models to produce time series with a strong common signal and
107 without biological persistence. These series may be more suitable to understand the effect of
108 climate on tree-growth, even if any persistence due to climate might be removed by pre-
109 whitening. For each chronology, the individual series were averaged to a single chronology by

110 computing the biweight robust means to reduce the influences of outliers (Cook et al. 1990b). In
111 this research we used residual chronologies obtained from ARSTAN to reconstruct temperature.
112
113 The mean sensitivity, which is a metric representing the year-to-year variation in ring width
114 (Fritts 1976), was calculated for each chronology and compared. The minimum sample depth for
115 each chronology was determined according to expressed population signal (EPS), which we used
116 as a guide for assessing the likely loss of reconstruction accuracy. Although arbitrary, we
117 required the commonly considered threshold of $EPS > 0.85$ (Wigley et al. 1984; Briffa & Jones
118 1990).

119

120 2.3 Temperature reconstruction

121

122 We extracted monthly temperature and precipitation records from the climate dataset CRU TS
123 3.23 gridded at 0.5° intervals (Jones and Harris 2008) from KNMI Climate Explorer
124 (<http://climexp.knmi.nl>) for $36\text{--}42^\circ\text{N}$, $26\text{--}38^\circ\text{E}$. The period AD 1930–2002 was chosen for the
125 analysis because it maximized the number of station records within the study area.

126

127 First, the climate-growth relationships were investigated with response function analysis (RFA)
128 (Fritts 1976) for biological year from previous October to current October using the
129 DENDROCLIM2002 program (Biondi & Waikul 2004). This analysis is done to determine the
130 months during which the tree-growth is the most responsive to temperature. Second, the climate
131 reconstruction is performed by regression based on the principal component (PCs) of the 23
132 chronologies within the study area. Principle Component Analysis (PCA) was done over the

133 entire period in common to the tree-ring chronologies. The significant PCs were selected by
134 stepwise regression. We combined forward selection with backward elimination setting $p \leq 0.05$
135 as entrance tolerance and $p \leq 0.1$ as exit tolerance. The final model obtained when the regression
136 reaches a local minimum of RMSE. The order of entry of the PCs into the model was PC₃, PC₂₁,
137 PC₄, PC₁₅, PC₅, PC₁₇, PC₇, PC₉, PC₁₀. The regression equation is calibrated on the common
138 period (1930–2002) between robust temperature time-series and the selected tree-ring series.
139 Third, the final reconstruction is based on bootstrap regression (Till and Guiot, 1990), a method
140 designed to calculate appropriate confidence intervals for reconstructed values and explained
141 variance even in cases of short time-series. It consists in randomly resampling the calibration
142 datasets to produce 1000 calibration equations based on a number of slightly different datasets.
143 The quality of the reconstruction is assessed by a number of standard statistics. The overall
144 quality of fit of reconstruction is evaluated based on the determination coefficient (R^2), which
145 expresses the percentage of variance explained by the model and the root mean squared error
146 (RMSE), which expresses the calibration error. This does not insure the quality of the
147 extrapolation which needs additional statistics based on independent observations, i.e.
148 observations not used by the calibration (verification data). They are provided by the
149 observations not resampled by the bootstrap process. The prediction RMSE (called RMSEP), the
150 reduction of error (RE) and the coefficient of efficiency (CE) are calculated on the verification
151 data and enable to test the predictive quality of the calibrated equations (Cook et al, 1994).
152 Traditionally, a positive RE or CE values means a statistically significant reconstruction model,
153 but bootstrap has the advantage to produce confidence intervals for such statistics without
154 theoretical probability distribution and finally we accept the RE and CE for which the lower
155 confidence margin at 95% are positive. This is more constraining than just accepting all positive

156 RE and CE. For additional verification, we also present traditional split-sample procedure results
157 that divided the full period into two subsets of equal length (*Meko and Graybill, 1995*).

158

159 To identify the extreme March–April cold and warm events in the reconstruction, standard
160 deviation (SD) values were used. Years one and two SD above and below the mean were
161 identified as warm, very warm, cold, and very cold years, respectively. Finally, as a way to
162 assess the spatial representation of our temperature reconstruction, we conducted a spatial field
163 correlation analysis between reconstructed values and the gridded CRU TS3.23 temperature field
164 (Jones and Harris 2008) for a broad region of the Mediterranean over the entire instrumental
165 period (ca. 1930–2002).

166

167 **3 Results and Discussion**

168 3.1 Tree-ring chronologies

169 In addition to 15 chronologies developed by previous studies, we produced six *P. nigra*, one *P.*
170 *sylvestris*, one *A. nordmanniana* / *P. orientalis* chronologies for this study (Table 2). The Çorum
171 district produced two *P. nigra* chronologies: one the longest (KAR; 627 years long) and the other
172 the most sensitive to climate (SAH; mean sensitivity value of 0.25). Previous investigations of
173 climate-tree growth relationships reported a mean sensitivity range of 0.13–0.25 for *P. nigra* in
174 Turkey (Köse 2011, Akkemik et al. 2008). The KAR, SAH, and ERC chronologies (with mean
175 sensitivity values from 0.22 to 0.25) were classified as very sensitive, and the SAV, HCR, and
176 PAY chronologies (mean sensitivity values range 0.17–0.18) contained values characteristic of
177 being sensitive to climate. The lowest mean sensitivity value was obtained for the ART A.

178 *nordmanniana* / *P. orientalis* chronology. Nonetheless, this chronology retained a statistically
179 significant temperature signal ($p < 0.05$).

180

181 3.2 March-April temperature reconstruction

182 RFA coefficients of May to August precipitation are positively correlated with most of the tree-
183 ring series (Fig. 2) and among them, May and June coefficients are generally significant. The
184 first principal component of the 23 chronologies, which explains 47% of the tree-growth
185 variance, is highly correlated with May–August total precipitation, statistically ($r = 0.65$, $p \leq$
186 0.001) and visually (Fig. 3). The high correlation was expected given that numerous studies also
187 found similar results in Turkey (Akkemik 2000a, Akkemik 2000b, Akkemik 2003, Akkemik et
188 al. 2005, Akkemik et al. 2008, Akkemik & Aras 2005, Hughes et al. 2001, D'Arrigo & Cullen
189 2001, Touchan et al. 2003; Touchan et al. 2005a, Touchan et al. 2005b, Touchan et al. 2007,
190 Köse et al. 2011, Köse et al. 2013, Martin-Benitto et al. 2016).

191

192 The influence of temperature was not as strong as May–August precipitation on radial growth,
193 although generally positive in early spring (March and April) (Fig. 2). Conversely, the ART
194 chronology from northeastern Turkey contained a strong temperature signal, which was
195 significantly positive in March. In addition to this chronology, we also used the chronologies that
196 revealed the influence of precipitation, as well as temperature to reconstruct March–April
197 temperature.

198

199 The higher order PCs of the 23 chronologies are significantly correlated with the March–April
200 temperature and, by nature, are independent on the precipitation signal (Table 3). The best

201 selection for fit temperature are obtained with the PC₃, PC₄, PC₅, PC₇, PC₉, PC₁₀, PC₁₅, PC₁₇,
202 PC₂₁, which explains together 25% of the tree-ring chronologies. So the temperature signal
203 remains important in the tree-ring chronologies and can be reconstructed. The advantage to
204 separate both signals through orthogonal PCs enable to remove an unwanted noise for our
205 temperature reconstruction. Thus, PC₁ was not used as potential predictor of temperature because
206 it is largely dominated by precipitation (Table 3, Fig. 3). The last two PCs contain a too small
207 part of the total variance to be used in the regressions. However, even if Jolliffe (1982) and Hadi
208 & Ling (1998) claimed that certain PCs with small eigenvalues (even the last one), which are
209 commonly ignored by principal components regression methodology, may be related to the
210 independent variable, we must be cautious with that because they may be much more dominated
211 by noise than the first ones. So, the contribution of each PC to the regression sum of squares is
212 also important for selection of PCs (Hadi & Ling 1998). The findings of Jolliffe (1982) and Hadi
213 & Ling (1998) provide a justification for using non-primary PCs, (*e.g.*, of second and higher
214 order) in our regression, given that correlations with temperature may be over-powered by
215 affects from precipitation in our study area (Cook 2011, personal communication).

216

217 Using this method, the calibration and verification statistics indicated a statistically significant
218 reconstruction (Table 4, Fig. 4). For additional verification, we also present split-sample
219 procedure results. Similarly bootstrap results, the derived calibration and verification tests using
220 this method indicated a statistically significant RE and CE values (Table 5).

221

222 The regression model accounted for 67% (Adj. $R^2 = 0.64$, $p \leq 0.0001$) of the actual temperature
223 variance over the calibration period (1930–2002). Also, actual and reconstructed March–April

224 temperature values had nearly identical trends during the period 1930–2002 (Fig. 4). Moreover, the tree-
225 ring chronologies successfully simulated both high frequency and warming trends in the temperature data
226 during this period. The reconstruction was more powerful at classifying warm events rather than cold
227 events. Over the last 73 years, eight of ten warm events in the instrumental data were also observed in
228 the reconstruction, while five of nine cold events were captured. Similarly, previous tree-ring based
229 precipitation reconstructions for Turkey (Köse et al. 2011; Akkemik et al. 2008) were generally
230 more successful in capturing dry years rather than wet years.

231

232 Our temperature reconstruction on the 1800–2002 period is obtained by bootstrap regression,
233 using 1000 iterations (Fig. 5). The confidence intervals are obtained from the range between the
234 2.5th and the 97.5th percentiles of the 1000 simulations. For the pre-instrumental period (1800–
235 1929), a total of 23 cold (1813, 1818, 1821, 1824, 1837, 1848, 1854, 1858, 1860, 1869, 1877–
236 1878, 1880–1881, 1883, 1897–1898, 1905–1907, 1911–1912, 1923) and 13 warm (1801–1802,
237 1807, 1845, 1853, 1866, 1872–1873, 1879, 1885, 1890, 1901, 1926) events were determined.

238 After comparing our results with event years obtained from May–June precipitation
239 reconstructions from western Anatolia (Köse et al. 2011), the cold years 1818, 1848, and 1897
240 appeared to coincide with wet years and 1881 was a very wet year for the entire region.

241 Furthermore, these years can be described as cold (in March–April) and wet (in May–June) for
242 western Anatolia.

243

244 Spatial correlation analysis revealed that our network-based temperature reconstruction was
245 representative of conditions across Turkey, as well as the broader Mediterranean region (Fig. 6).

246 During the period 1930–2002, estimated temperature values were highly significant (r range 0.5–

247 0.6, $p < 0.01$) with instrumental conditions recorded from southern Ukraine to the west across
248 Romania, and from northern areas of Libya and Egypt to the east across Iraq. The strength of the
249 reconstruction model is evident in the broad spatial implications demonstrated by the
250 temperature record. Thus, we interpret warm and cold periods and extreme events within the
251 record with high confidence.

252

253 Among the warm periods in our reconstruction, conditions during the year 1879 were dry, 1895
254 wet, and 1901 very wet across the broad region of western Anatolia (Köse et al. 2011). Hence,
255 we defined 1879 as a warm (in March–April) and dry year (in May–June), and 1895 and 1901
256 were warm and wet years. In the years 1895 and 1901 the combination of a warm early spring
257 and a wet late spring-summer caused enhanced radial growth in Turkey, interpreted as longer
258 growing seasons without drought stress.

259

260 Of these event years, 1897 and 1898 were exceptionally cold and 1845, 1872 and 1873 were
261 exceptionally warm. During the last 200 years, our reconstruction suggests that the coldest year
262 was 1898 and the warmest year was 1873. The reconstructed extreme events also coincided with
263 accounts from historical records. Server (2008) recounted the winter of 1898 as characterized by
264 anomalously cold temperatures that persisted late into the spring season. A family, who brought
265 their livestock herds up into the plateau region in Kırşehir seeking food and water were suddenly
266 covered in snow on 11 March 1898. This account of a late spring freeze supports the
267 reconstruction record of spring temperatures across Turkey, and offers corroboration to the
268 quality of the reconstructed values.

269

270 Seyf (1985) reported that extreme summer temperature during the year 1873 resulted in
271 widespread crop failure and famine. Historical documents recorded an infamous drought-derived
272 famine that occurred in Anatolia from 1873 to 1874 (Quataert, 1996, Kuniholm, 1990), which
273 claimed the lives of 250,000 people and a large number of cattle and sheep (Faroqhi, 2009). This
274 drought caused widespread mortality of livestock and depopulation of rural areas through human
275 mortality, and migration of people from rural to urban areas. Further, the German traveler
276 Naumann (1893) reported a very dry and hot summer in Turkey during the year 1873 (Heinrich
277 et al, 2013). Conditions worsened when the international stock exchanges crashed in 1873,
278 marking the beginning of the "Great Depression" in the European economy (Zürcher, 2004). Our
279 temperature record suggests that dry conditions during the early 1870s were possibly exacerbated
280 by warm spring temperatures that likely carried into summer. A similar pattern of intensified
281 drought by warm temperatures was demonstrated recently by Griffin and Anchukaitis (2014) for
282 the current drought in California, USA.

283

284 Extreme cold and warm events were usually one year long, and the longest extreme cold and
285 warm events were two and three years, respectively. These results were similar with durations of
286 extreme wet and dry events in Turkey (Touchan et al. 2003, Touchan et al. 2005a, Touchan et al.
287 2005b, Touchan et al. 2007, Akkemik & Aras, 2005, Akkemik et al. 2005, Akkemik et al. 2008,
288 Köse et al. 2011). Moreover, seemingly innocuous short-term warm events, such as the 1807
289 event, were recorded across the Mediterranean and in high elevations of the European regions.
290 Casty et al. (2005) reported the year 1807 as being one of the warmest alpine summers in the
291 European Alps over the last 500 years. As such, a drought record from Nicault et al. (2008)

292 echoes this finding, as a broad region of the Mediterranean basin experienced drought
293 conditions.

294

295 Low frequency variability of our spring temperature reconstruction showed larger variability in
296 nineteenth century than twentieth century. Similar results observed on previous tree-ring based
297 precipitation reconstructions from Turkey (Touchan et al. 2003, D'Arrigo et al. 2001, Akkemik
298 and Aras 2005, Akkemik et al. 2005, Köse et al. 2011). Moreover, cold periods observed in our
299 reconstruction are generally appeared as generally wet in the precipitation reconstructions, while
300 warm periods generally correlated with dry periods (Fig. 7).

301

302 Heinrich et al. (2013) analyzed winter-to-spring (January–May) air temperature variability in
303 Turkey since AD 1125 as revealed from a robust tree-ring carbon isotope record from *Juniperus*
304 *excelsa*. Although they offered a long-term perspective of temperature over Turkey, the
305 reconstruction model, which covered the period 1949–2006, explained 27% of the variance in
306 temperature since the year 1949. In this study, we provided a short-term perspective of
307 temperature fluctuation based on a robust model (calibrated and verified 1930–2002; Adj. $R^2 =$
308 0.64 ; $p \leq 0.0001$). Yet, the Heinrich et al. (2013) temperature record did not capture the 20th
309 century warming trend as found elsewhere (Wahl et al. 2010). However, their temperature trend
310 does agree with trend analyses conducted on meteorological data from Turkey and other areas in
311 the eastern Mediterranean region. The warming trend seen during our reconstruction calibration
312 period (1930–2002) was similar to the data shown by Wahl et al. (2010) across the region and
313 hemisphere. Further, the warming trends seen in our record agrees with data presented by Turkes
314 & Sumer (2004), of which they attributed to increased urbanization in Turkey. Considering long-

315 term changes in spring temperatures, the 19th century was characterized by more high-frequency
316 fluctuations compared to the 20th century, which was defined by more gradual changes and
317 includes the beginning of decreased DTRs in the region (Turkes & Sumer, 2004).

318

319 **4 Conclusions**

320

321 In this study, we used a broad network of tree-ring chronologies to provide the first tree-ring
322 based temperature reconstruction for Turkey and identified extreme cold and warm events during
323 the period 1800–1929 CE. Similar to the precipitation reconstructions against which we compare
324 our air temperature record, extreme cold and warm years were generally short in duration (one
325 year) and rarely exceeded two-three years in duration. The coldest and warmest years over
326 western Anatolia were experienced during the 19th century, and the 20th century is marked by a
327 temperature increase.

328

329 Reconstructed temperatures for the 19th century suggest that more short-term fluctuations
330 occurred compared to the 20th century. The gradual warming trend shown by our reconstruction
331 calibration period (1930–2002) is coeval with decreases in spring DTRs. Given the results of
332 Turkes and Sumer (2004), the variations in short- and long-term temperature changes between
333 the 19th and 20th centuries might be related to increased urbanization in Turkey.

334

335 The study revealed the potential for reconstructing temperature in an area previously thought
336 impossible, especially given the strong precipitation signals displayed by most tree species
337 growing in the dry Mediterranean climate that characterizes broad areas of Turkey. Our

338 reconstruction only spans 205 years due to the shortness of the common interval for the
339 chronologies used in this study, but the possibility exists to extend our temperature
340 reconstruction further back in time by increasing the sample depth with more temperature-
341 sensitive trees, especially from northeastern Turkey. Thus future research will focus on
342 increasing the number of tree-ring sites across Turkey, and maximizing chronology length at
343 existing sites that would ultimately extend the reconstruction back in time.

344

345 **Acknowledgements**

346

347 This research was supported by The Scientific and Technical Research Council of Turkey
348 (TUBITAK); Projects ÇAYDAG 107Y267 and YDABAG 102Y063. N. Köse was supported by
349 The Council of Higher Education of Turkey. We are grateful to the Turkish Forest Service
350 personnel and Ali Kaya, Umut Ç. Kahraman and Hüseyin Yurtseven for their invaluable support
351 during our field studies. J. Guiot was supported by the Labex OT-Med (ANR-11-LABEX-0061),
352 French National Research Agency (ANR).

353

354 **References**

- 355 Akkemik, Ü.: Dendroclimatology of Umbrella pine (*Pinus pinea* L.) in Istanbul (Turkey), Tree-
356 Ring Bull., 56, 17–20, 2000a.
- 357 Akkemik, Ü.: Tree-ring chronology of *Abies cilicica* Carr. in the Western Mediterranean Region
358 of Turkey and its response to climate, Dendrochronologia, 18, 73–81, 2000b.
- 359 Akkemik, Ü.: Tree-rings of *Cedrus libani* A. Rich the northern boundary of its natural
360 distribution, IAWA J, 24(1), 63-73, 2003.
- 361 Akkemik, Ü. and Aras, A.: Reconstruction (1689–1994) of April–August precipitation in
362 southwestern part of central Turkey, Int. J. Clim., 25, 537–548, 2005.
- 363 Akkemik, Ü., Dagdeviren, N., and Aras, A.: A preliminary reconstruction (A.D. 1635–2000) of
364 spring precipitation using oak tree rings in the western Black Sea region of Turkey, Int. J.
365 Biomet., 49(5), 297–302, 2005.
- 366 Akkemik, Ü., D’Arrigo, R., Cherubini, P., Köse, N., and Jacoby, G.: Tree-ring reconstructions of
367 precipitation and streamflow for north-western Turkey, Int. J. Clim., 28, 173–183, 2008.
- 368 Biondi, F. and Waikul, K.: DENDROCLIM2002: A C++ program for statistical calibration of
369 climate signals in tree-ring chronologies, Comp. Geosci., 30, 303–311, 2004.
- 370 Briffa, K. R. and Jones, P. D.: Basic chronology statistics and assessment. In: Methods of
371 Dendrochronology: Applications in the Environmental Sciences (Cook, E. and Kairiukstis, L.
372 A. eds). Kluwer Academic Publishers, Amsterdam, pp. 137–152, 1990.
- 373 Casty, C., Wanner, H., Luterbacher, J., Esper, J., and Böhm, R.: Temperature and precipitation
374 variability in the European Alps since 1500, Int. J. Clim., 25(14), 1855–1880, 2005.

375 Cook, E.: A time series analysis approach to tree-ring standardization. PhD. Dissertation.
376 University of Arizona, Tucson, 1985.

377 Cook, E., Briffa, K., Shiyatov, S., and Mazepa, V.: Tree-ring standardization and growth-trend
378 estimation. In: *Methods of Dendrochronology: Applications in the Environmental Sciences*
379 (Cook, E. and Kairiukstis, L. A. eds). Kluwer Academic Publishers, Amsterdam, pp.104–
380 122, 1990a.

381 Cook, E., Shiyatov, S., and Mazepa, V.: Estimation of the mean chronology. In: *Methods of*
382 *Dendrochronology: Applications in the Environmental Sciences* (Cook, E. and Kairiukstis, L.
383 A. eds). Kluwer Academic Publishers, Amsterdam, pp. 123–132, 1990b.

384 D'Arrigo, R. and Cullen, H. M.: A 350-year (AD 1628–1980) reconstruction of Turkish
385 precipitation. *Dendrochronologia* ,19(2), 169–177, 2001.

386 Deniz, A., Toros, T., and Incecik, S.: Spatial variations of climate indices in Turkey, *Int. J.*
387 *Clim.*, 31, 394-403, 2011.

388 Fritts, H. C.: *Tree Rings and Climate*. Academic Press, New York, 1976.

389 Griggs, C., DeGaetano, A., Kuniholm, P., and Newton, M.: A regional high-frequency
390 reconstruction of May–June precipitation in the north Aegean from oak tree rings, A.D.
391 1809–1989, *Int. J. Clim.*, 27, 1075–1089, 2007.

392 Grissino-Mayer, H. D.: Evaluating crossdating accuracy: A manual and tutorial for the computer
393 program COFECHA, *Tree-Ring Res.*, 57, 205–221, 2001.

394 Griffin, D. and Anchukaitis, K. J.: How unusual is the 2012–2014 California drought? *Geophy.*
395 *Res. Lett.*, 41(24), 9017–9023, 2014.

396 Hadi, A. S. and Ling, R. F.: Some cautionary notes on the use of principal components
397 regression, *Amer. Statist.*, 52(1), 15–19, 1998.

398 Heinrich, I., Touchan, R., Liñán, I. D., Vos, H., and Helle, G.: Winter-to-spring temperature
399 dynamics in Turkey derived from tree rings since AD 1125, *Clim. Dynam.*, 41(7–8), 1685–
400 1701, 2013.

401 Holmes, R. L.: Computer-assisted quality control in tree-ring data and measurements, *Tree-Ring*
402 *Bull.*, 43, 69–78, 1983.

403 Hughes, M. K., Kuniholm, P. I., Garfin, G. M., Latini, C., and Eischeid, J.: Aegean tree-ring
404 signature years explained, *Tree-Ring Res.*, 57(1), 67–73, 2001.

405 Jolliffe, I. T.: A note on the use of principal components in regression, *Appl. Stat.*, 31(3), 300–
406 303, 1982.

407 Jones, P. D. and Harris, I.: Climatic Research Unit (CRU) time-series datasets of variations in
408 climate with variations in other phenomena. NCAS British Atmospheric Data Centre, 2008.
409 <http://catalogue.ceda.ac.uk/uuid/3f8944800cc48e1cbc29a5ee12d8542d>

410 Köse, N., Akkemik, Ü., and Dalfes, H. N.: Anadolu'nun iklim tarihinin son 500 yılı:
411 Dendroklimatolojik ilk sonuçlar. Türkiye Kuvaterner Sempozyumu-TURQUA-V, 02–03
412 Haziran 2005, *Bildiriler Kitabı*, 136–142 (In Turkish), 2005.

413 Köse, N., Akkemik, Ü., Dalfes, H. N., and Özeren, M. S.: Tree-ring reconstructions of May–June
414 precipitation of western Anatolia, *Quat. Res.*, 75, 438–450, 2011.

415 Köse N., Akkemik U., Guner H.T., Dalfes H.N., Grissino-Mayer H.D., Ozeren M.S., Kindap T.
416 (2013) An improved reconstruction of May– June precipitation using tree-ring data from
417 western Turkey and its links to volcanic eruptions, *Int. J. Biometeorol.*, 57(5):691–701

418 Martin-Benito, D., Ummenhofer C.C., Köse, N., Güner, H.T., Pederson, N. 2016. Tree-ring
419 reconstructed May-June precipitation in the Caucasus since 1752 CE, *Clim. Dyn.*, DOI
420 10.1007/s00382-016-3010-1.

421 Meko, D. M. and Graybill, D. A.: Tree-ring reconstruction of upper Gila River discharge, *Wat.*
422 *Res. Bull.*, 31, 605–616, 1995.

423 Mutlu, H., Köse, N., Akkemik, Ü., Aral, D., Kaya, A., Manning, S. W., Pearson, C. L., and
424 Dalfes, N.: Environmental and climatic signals from stable isotopes in Anatolian tree rings,
425 Turkey, *Reg. Environ. Change*, doi: 10.1007/s1011301102732, 2011.

426 Nicault, A., Alleaume, S., Brewer, S., Carrer, M., Nola, P., and Guiot, J.: Mediterranean drought
427 fluctuation during the last 500 years based on tree-ring data, *Clim. Dynam.*, 31(2–3), 227–
428 245, 2008.

429 Orvis, K. H. and Grissino-Mayer, H. D.: Standardizing the reporting of abrasive papers used to
430 surface tree-ring samples, *Tree-Ring Res.*, 58, 47–50, 2002.

431 Server, M.: Evaluation of an oral history text in the context of social memory and traditional
432 activity, *Milli Folklor* 77, 61–68 (In Turkish), 2008.

433 Speer, J. H.: *Fundamentals of Tree-Ring Research*, University of Arizona Press, Tucson, 2010.

434 Stokes, M. A. and Smiley, T. L.: *An Introduction to Tree-ring Dating*, The University of Arizona
435 Press, Tucson, 1996.

436 Till, C. and Guiot, J.: Reconstruction of precipitation in Morocco since A D 1100 based on
437 *Cedrus atlantica* tree-ring widths, *Quat. Res.*, 33, 337–351, 1990.

438 Touchan, R., Garfin, G. M., Meko, D. M., Funkhouser, G., Erkan, N., Hughes, M. K., and
439 Wallin, B. S.: Preliminary reconstructions of spring precipitation in southwestern Turkey
440 from tree-ring width, *Int. J. Clim.*, 23, 157–171, 2003.

441 Touchan, R., Xoplaki, E., Funkhouser, G., Luterbacher, J., Hughes, M. K., Erkan, N., Akkemik,
442 Ü., and Stephan, J.: Reconstruction of spring/summer precipitation for the Eastern
443 Mediterranean from tree-ring widths and its connection to large-scale atmospheric
444 circulation, *Clim. Dynam.*, 25, 75–98, 2005a.

445 Touchan, R., Funkhouser, G., Hughes, M. K., and Erkan, N.: Standardized Precipitation Index
446 reconstructed from Turkish ring widths, *Clim. Change*, 72, 339–353, 2005b.

447 Touchan, R., Akkemik, Ü., Huges, M. K., and Erkan, N.: May–June precipitation reconstruction
448 of southwestern Anatolia, Turkey during the last 900 years from tree-rings, *Quat. Res.*, 68,
449 196–202, 2007.

450 Turkes, M.: Spatial and temporal analysis of annual rainfall variations in Turkey. *Int. J. Clim.*,
451 16, 1057–1076, 1996.

452 Turkes, M.: Vulnerability of Turkey to desertification with respect to precipitation and aridity
453 conditions. *Turk. J. Engineer. Environ Sci.*, 23, 363–380, 1999.

454 Turkes, M. and Sumer, U. M.: Spatial and temporal patterns of trends variability in diurnal
455 temperature ranges of Turkey. *Theor. Appl. Clim.*, 77, 195–227, 2004.

456 Wahl, E. R., Anderson, D. M., Bauer, B. A., Buckner, R., Gille, E. P., Gross, W. S., Hartman,
457 M., and Shah, A.: An archive of high-resolution temperature reconstructions over the past
458 two millennia, *Geochem. Geophys. Geosyst.*, 11, Q01001, doi:10.1029/2009GC002817,
459 2010.

460 Wigley, T. M. L., Briffa, K. R., and Jones, P. D.: On the average value of correlated time series
461 with applications in dendroclimatology and hydrometeorology, *J. Clim. Appl. Met.*, 23, 201–
462 213, 1984.

463 Yamaguchi, D. K.: A simple method for cross-dating increment cores from living trees. *Can. J.*
464 *For. Res.*, 21, 414–416, 1991.

465 Table 1. Site information for the new chronologies developed by this study in Turkey.

| Site name | Site code | Species | No. trees/ cores | Aspect | Elev. (m) | Lat. (N) | Long. (E) |
|---|-----------|--|---------------------|--------|---------------|-------------|--------------|
| Çorum, Kargı, Karakise kayalıkları | KAR | <i>Pinus nigra</i> | 22 / 38 | SW | 1522 | 41°11' | 34°28' |
| Çorum, Kargı, Şahinkayası mevki | SAH | <i>P. nigra</i> | 12 / 21 | S | 1300 | 41°13' | 34°47' |
| Bilecik, Muratdere | ERC | <i>P. nigra</i> | 12 / 25 | SE | 1240 | 39°53' | 29°50' |
| Bolu, Yedigöller, Ayıkaya mevki | BOL | <i>P. sylvestris</i> | 10 / 20 | SW | 1702 | 40°53' | 31°40' |
| Eskişehir, Mihalıççık, Savaş alanı mevkii | SAV | <i>P. nigra</i> | 10 / 18 | S | 1558 | 39°57' | 31°12' |
| Kayseri, Aladağlar milli parkı, Hacer ormanı | HCR | <i>P. nigra</i> | 18 / 33 | S | 1884 | 37°49' | 35°17' |
| Kahramanmaraş, Göksun, Payanburnu mevkii | PAY | <i>P. nigra</i> | 10 / 17 | S | 1367 | 37°52' | 36°21' |
| Artvin, Borçka, Balcı işletmesi | ART | <i>Abies nordmanniana</i> <i>Picea orientalis</i> | 23 / 45 | N | 1200– 2100 | 41°18' | 41°54' |

466

467

468 Table 2. Summary statistics for the new chronologies developed by this study in Turkey.

| Site Code | Total chronology | | | Common interval | | |
|-----------|------------------|------------------------|------------------|-----------------|--|-------------------------------|
| | Time span | 1st year (*EPS > 0.85) | Mean sensitivity | Time span | Mean correlations: among radii /between radii and mean | Variance explained by PC1 (%) |
| KAR | 1307–2003 | 1620 | 0.22 | 1740–1994 | 0.38 / 0.63 | 41 |
| SAH | 1663–2003 | 1738 | 0.25 | 1799–2000 | 0.42 / 0.67 | 45 |
| ERC | 1721–2008 | 1721 | 0.23 | 1837–2008 | 0.45 / 0.69 | 48 |
| BOL | 1752–2009 | 1801 | 0.18 | 1839–1994 | 0.32 / 0.60 | 36 |
| SAV | 1630–2005 | 1700 | 0.17 | 1775–2000 | 0.33 / 0.60 | 38 |
| HCR | 1532–2010 | 1704 | 0.18 | 1730–2010 | 0.38 / 0.63 | 40 |
| PAY | 1537–2010 | 1790 | 0.18 | 1880–2010 | 0.28 / 0.56 | 32 |
| ART | 1498–2007 | 1624 | 0.12 | 1739–1996 | 0.37 / 0.60 | 41 |

469 *EPS = Expressed Population Signal [Wigley et al., 1984]

470

471 Table 3. Statistics from reconstruction model principal components analysis.

| | Explained variance (%) | Correlation coefficients with | | The chronologies represented by higher magnitudes** in the eigenvectors |
|-------|------------------------|-------------------------------|-----------------|---|
| | | May–August PPT | March–April TMP | |
| PC1 | 46.57 | 0.65 | 0.19 | KAR, KIZ, TEF, BON, USA, TUR, CAT, INC, ERC, YAU, SAV, TAN, SIU |
| PC2 | 7.86 | -0.07 | 0.15 | KAR, SAV, TIR, BOL, YAU, ESK, TEF, BON, SIU |
| PC3* | 4.93 | 0.04 | -0.48 | HCR, PAY, BOL, YAU, SIA |
| PC4* | 4.68 | 0.11 | 0.17 | TEF, KEL, FIR, SIA, KIZ, SIU, ART |
| PC5* | 4.42 | -0.25 | 0.27 | SAH, TIR, FIR, ART |
| PC6 | 3.73 | 0.15 | -0.14 | KIZ, FIR, SAV, KAR, TIR, PAY, ESK, TEF, BON, ART |
| PC7* | 3.56 | 0.19 | 0.18 | KIZ, BON, BOL, YAU, HCR, PAY, INC |
| PC8 | 2.87 | 0.26 | 0.01 | HCR, ESK, BON, FIR, ERC, SIA |
| PC9* | 2.45 | 0.16 | 0.17 | PAY, USA, BOL, YAU, TIR, HCR, FIR, SIA, SIU |
| PC10* | 2.21 | 0.14 | -0.08 | TUR, CAT, SAV, SIA, KEL, ERC, SIU |
| PC11 | 2.09 | -0.36 | -0.20 | HCR, TEF, USA, INC, PAY, TUR, SAV, SIU |
| PC12 | 1.80 | -0.12 | 0.05 | TEF, CAT, YAU, HCR, ESK, USA, BOL, SIA |
| PC13 | 1.63 | -0.06 | 0.17 | TEF, TUR, BOL, KAR, YAU, SIA |
| PC14 | 1.55 | -0.14 | 0.06 | TIR, USA, FIR, TUR, YAU, KAR, BON |
| PC15* | 1.50 | -0.20 | -0.14 | KIZ, BON, USA, ESK, INC, BOL |
| PC16 | 1.31 | 0.04 | 0.08 | SAH, HCR, INC, YAU, SAV, KAR, FIR, BOL, SIU |
| PC17* | 1.25 | 0.15 | 0.19 | SAH, SIU, KAR, ESK, TUR, ERC |
| PC18 | 1.14 | 0.13 | 0.02 | KAR, TEF, TUR, SAV, BON, CAT |
| PC19 | 1.09 | 0.16 | -0.11 | PAY, INC, SAV, HCR, KEL, CAT, TAN |
| PC20 | 0.95 | -0.15 | -0.01 | TIR, SAH, CAT |
| PC21* | 0.89 | 0.06 | -0.28 | TUR, INC, TIR, SAV |
| PC22 | 0.85 | 0.44 | 0.10 | KIZ, SAH, BON, YAU, SIU |
| PC23 | 0.67 | -0.22 | -0.02 | TAN, KEL, TUR, CAT |

472 “*” indicates the PCs, which used in the reconstruction as predictors

473 “**” which exceed ± 0.2 value.

474

475

476

477

478

479 Table 4. Calibration and verification statistics of bootstrap method (1000 iterations

480 applied) showing the mean values based on the 95% confidence interval (CI)

481

| | | Mean (95% CI) |
|--------------|-------|-------------------|
| Calibration | RMSE | 0.65 (0.52; 0.77) |
| | R^2 | 0.73 (0.60; 0.83) |
| Verification | RE | 0.54 (0.15; 0.74) |
| | CE | 0.51 (0.04; 0.72) |
| | RMSEP | 0.88 (0.67; 1.09) |

482 *RMSE* root mean squared error; R^2 coefficient of determination; *RE* reduction of error; *CE*

483 coefficient of efficiency; *RMSEP* root mean squared error prediction

484

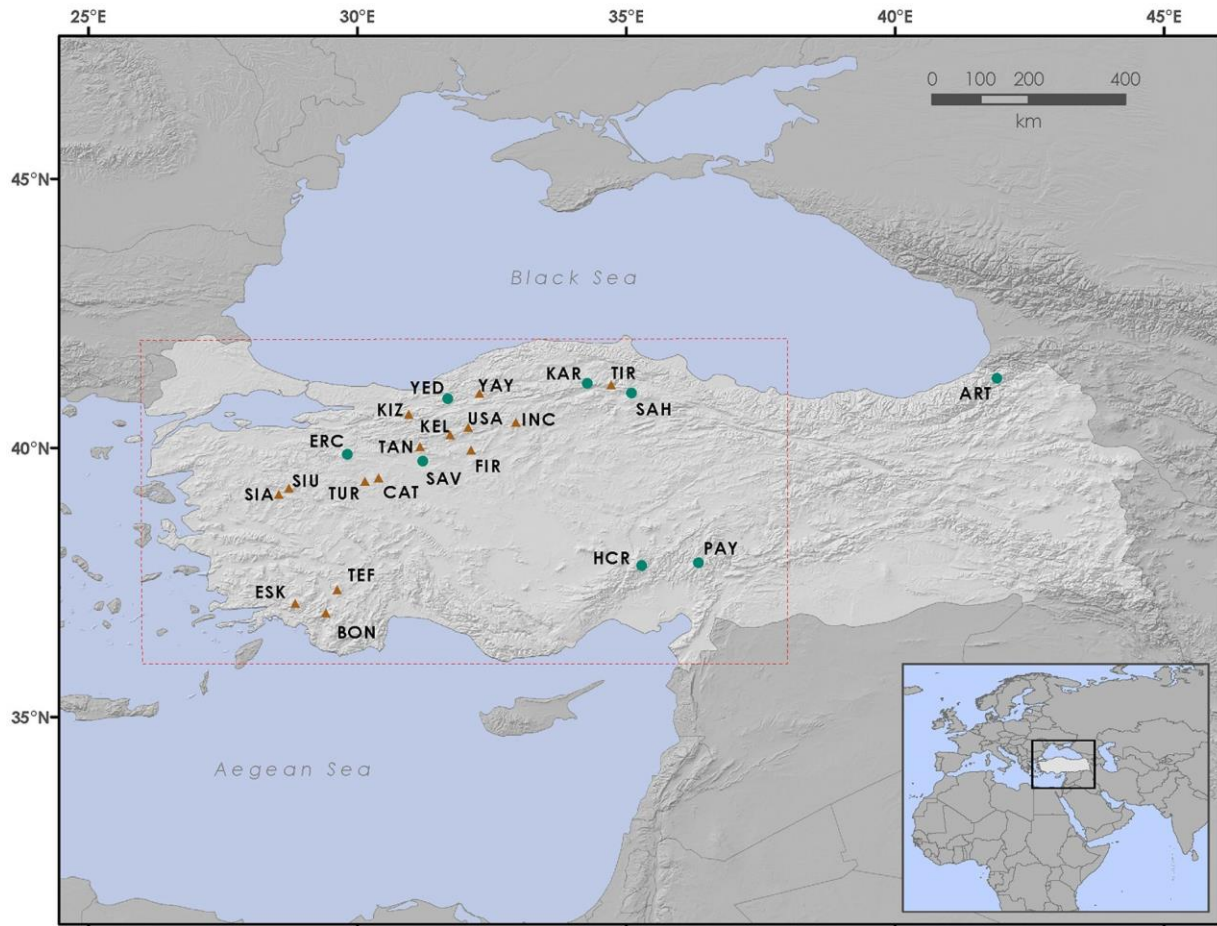
485 Table 5. Results of the statistical calibrations and cross-validations

| Calibration Period | Verification Period | Adj. R^2 | F | RE | CE |
|-----------------------|------------------------|------------|-----------------|------|------|
| 1930–1966 | 1967–2002 | 0.55 | 5.91 | 0.64 | 0.58 |
| | | | $p \leq 0.0001$ | | |
| 1967–2002 | 1930–1966 | 0.71 | 10.45 | 0.63 | 0.46 |
| | | | $p \leq 0.0001$ | | |

486

487

488

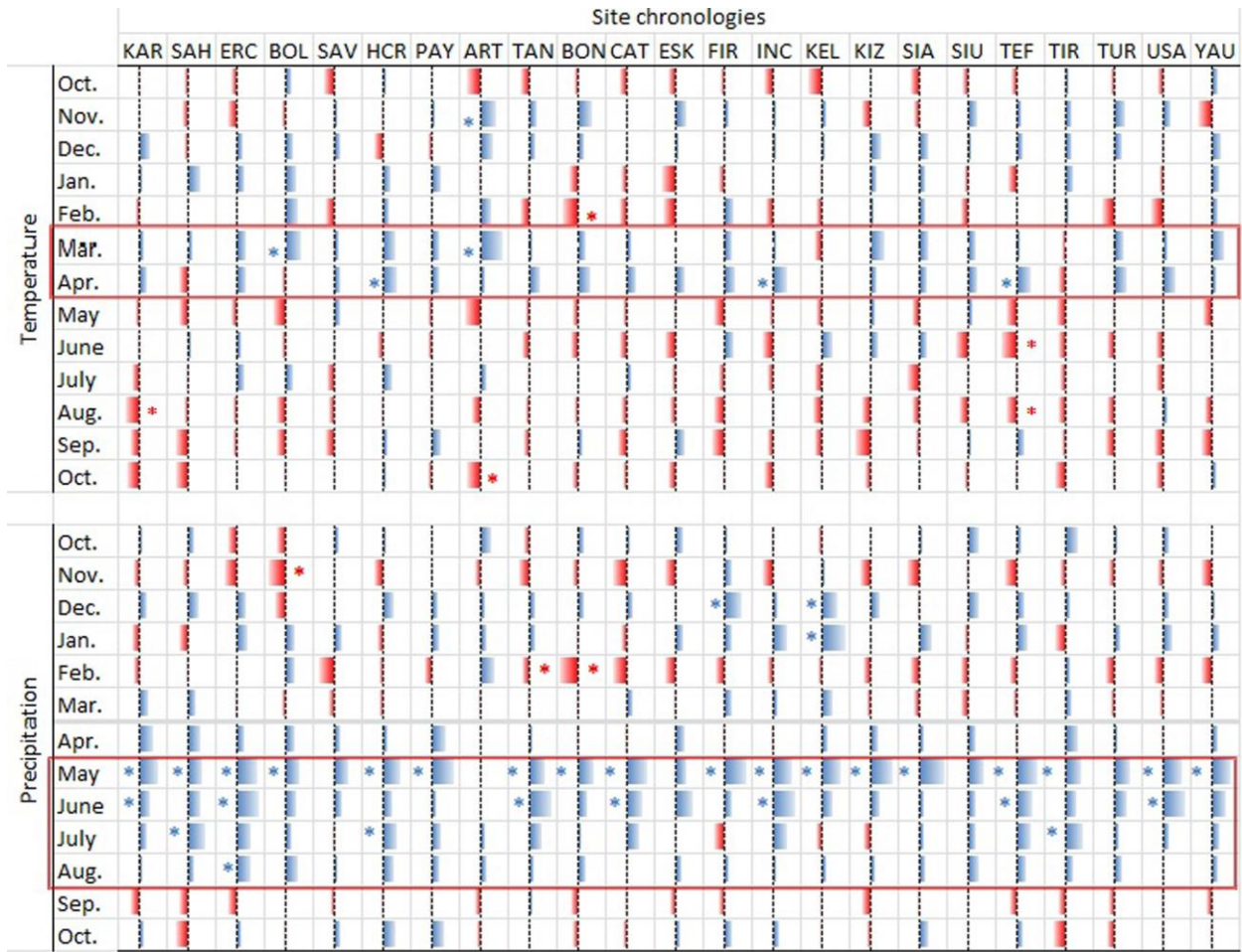


489
 490 **Figure 1.** Tree-ring chronology sites in Turkey used to reconstruct temperature. Circles
 491 represent the new sampling efforts from this study and the triangles represent previously-
 492 published chronologies (YAY, SIA, SIU: Mutlu et al. 2011; TIR: Akkemik et al. 2008; TAN:
 493 Köse et al. unpublished data; KIZ, ESK, TEF, BON, KEL, USA, FIR, TUR: Köse et al. 2011;
 494 CAT, INC: Köse et al. 2005). The box (dashed line) represents the area for which the
 495 temperature reconstruction was performed.

496

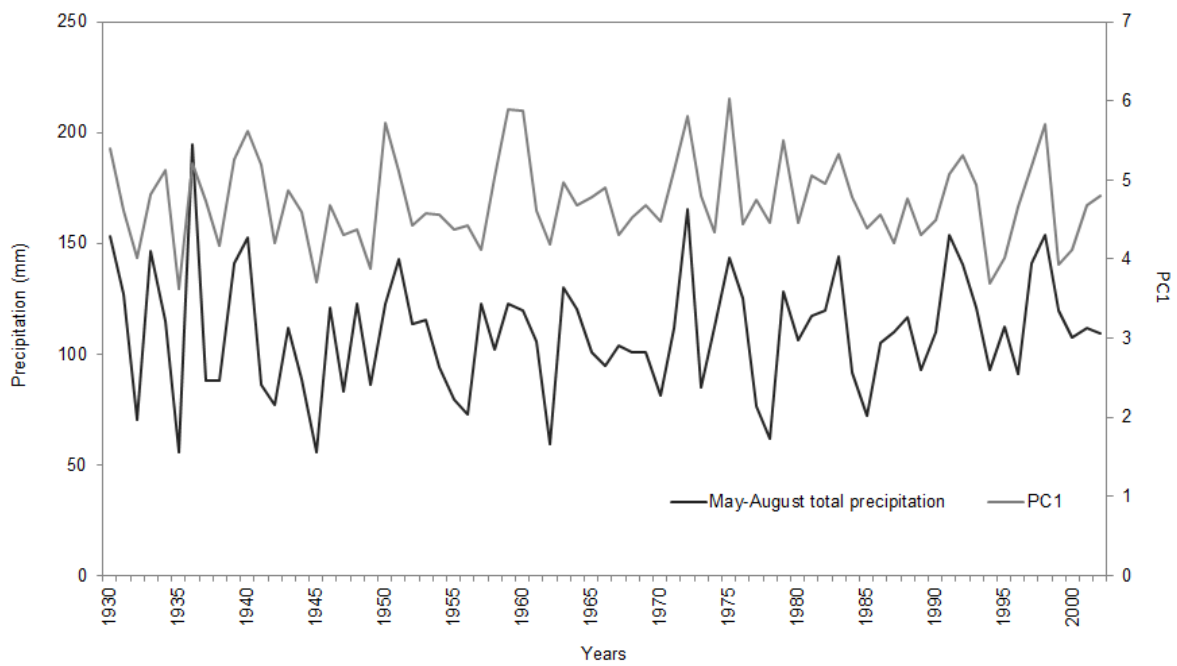
497

498



499

500 **Figure 2.** Summary of response function results of 23 chronologies. Red color represents
 501 negative effects of climate variability on tree ring width; blue color represents positive effects of
 502 climate variability on tree ring width. “*” indicates statistically significant response function
 503 confidents ($p \leq 0.05$). Each response function includes 13 weights for average monthly
 504 temperatures and 13 monthly precipitations from October of the prior year to October of current
 505 year.



506

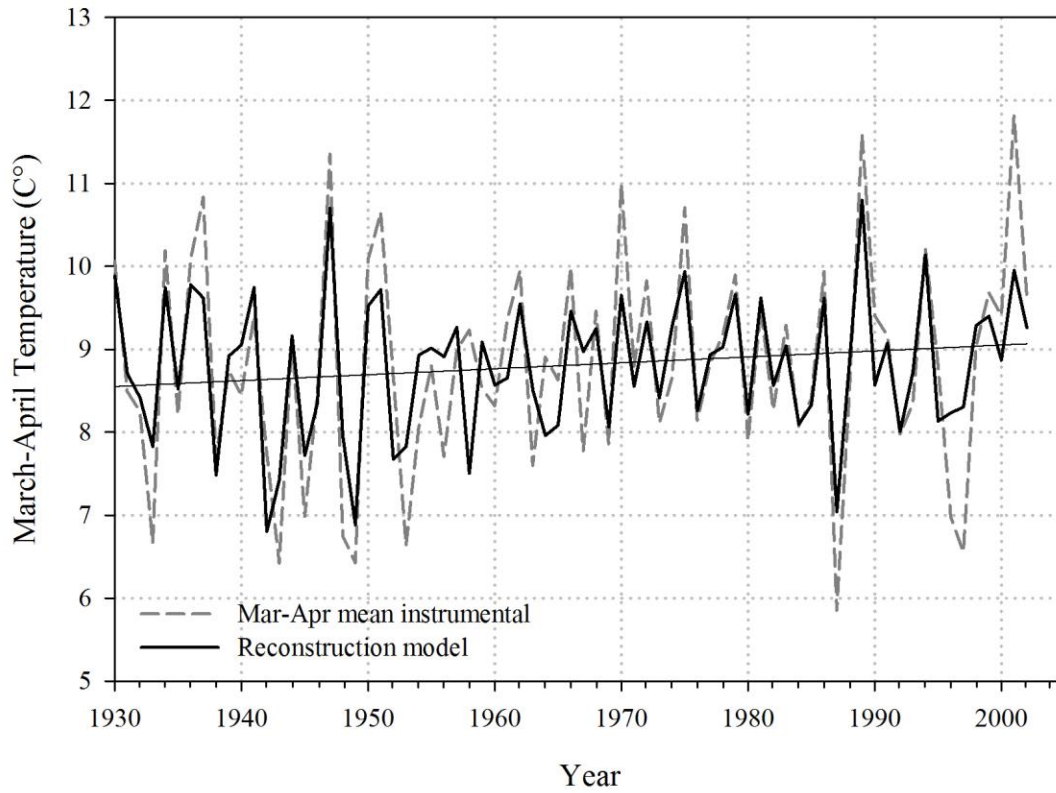
507 **Figure 3.** The comparison of May-August total precipitation (mm) and the first principal
 508 component of 23 tree-ring chronologies.

509

510

511

512



513

514 **Figure 4.** Actual (instrumental) and reconstructed March–April temperature (°C). Dashed lines
 515 (dark grey) represent actual values and solid lines (black) represent reconstructed values shown
 516 with trend line (linear black line). Note: y-axes labels range 5–13 °C.

517

518

519

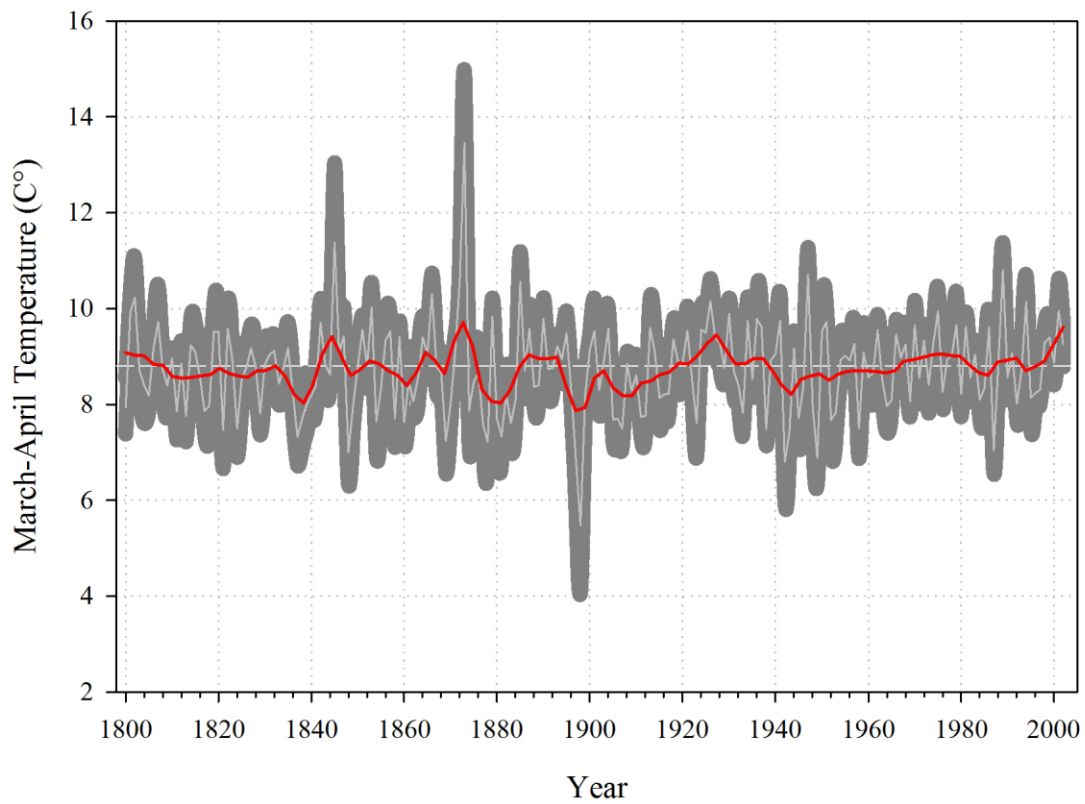
520

521

522

523

524



525

526 **Figure 5.** March–April temperature reconstruction for Turkey for the period 1800–2002

527 CE. The central horizontal line (dashed white) shows the reconstructed long-term mean;

528 dark grey background denotes Monte Carlo ($n = 1000$) bootstrapped 95% confidence

529 limits; and the solid black line shows 13-year low-pass filter values. Note: y-axis labels

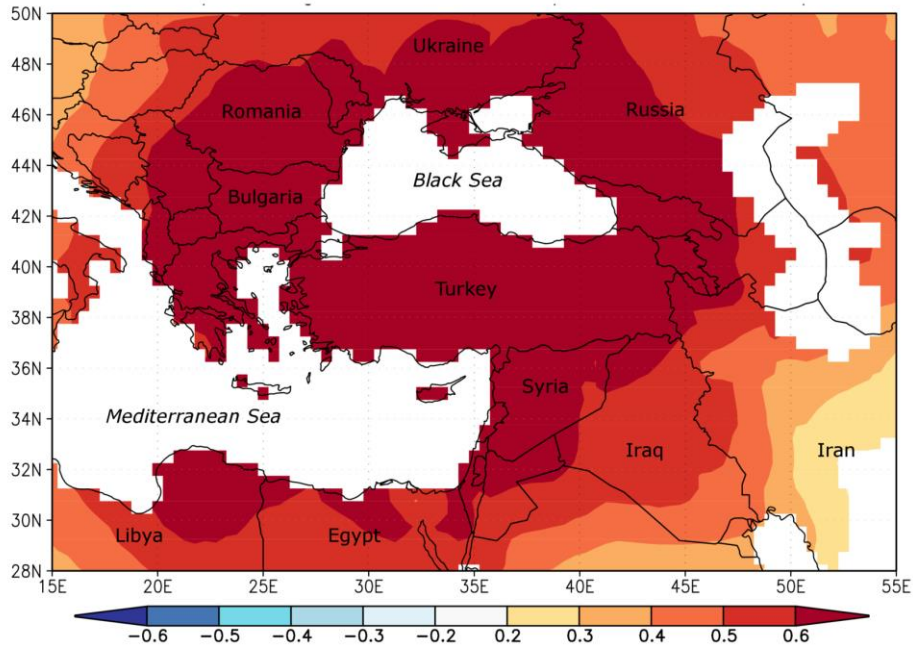
530 range 2–16 °C.

531

532

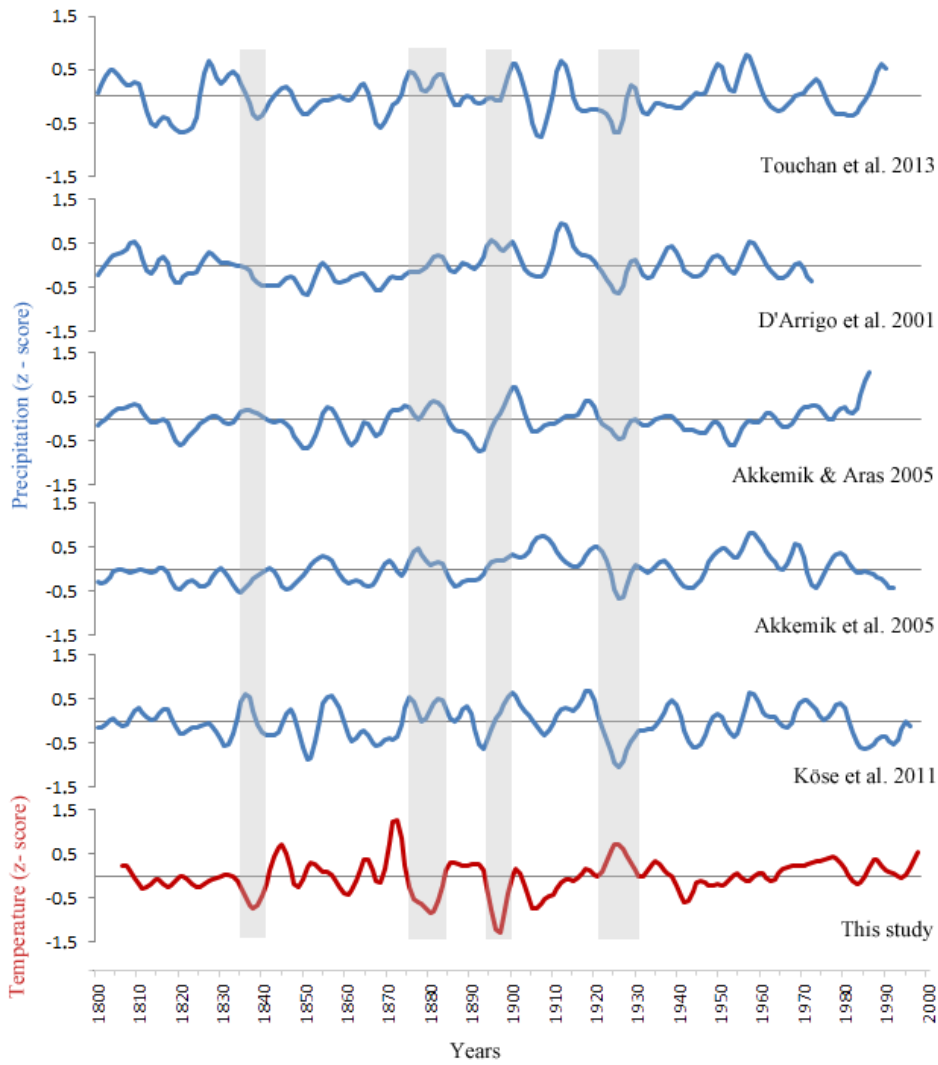
533

534



535

536 **Figure 6.** Spatial correlation map for the March–April temperature reconstruction. Spatial
 537 field correlation map showing statistical relationship between the temperature
 538 reconstruction and the gridded temperature field at 0.5° intervals (CRU TS3.23; Jones and
 539 Harris 2008) during the period 1930–2002 over the Mediterranean region.



540

541 **Figure 7.** Low-frequency variability of previous tree-ring based precipitation
 542 reconstructions from Turkey and spring temperature reconstruction. Each line shows 13-
 543 year low-pass filter values. z-scores were used for comparison.

544